Potential Energy Surface Crossings in Organic Photochemistry

Fernando Bernardi and Massimo Olivucci
Dipartimento di Chimica "G. Ciamician" dell'Università di Bologna, Via Selmi 2, 40126 Bologna, Italy

Michael A. Robb
Department of Chemistry, King's College, London, Strand, London, UK WC2R 2LS

1 Introduction

As a result of complementary experimental and theoretical work in the last five years, new aspects of the excited state behaviour of organic molecules have emerged. The most general of these is that low-lying intersections (crossings) between the photochemically relevant excited state and the ground state occur with a previously unsuspected frequency. Thus, an organic molecule moving on an excited state potential energy surface has a high probability of entering a region of surface crossing during the excited state lifetime. Such crossings, conical intersections in the case of two singlet (or two triplet) surfaces, or singlet–triplet surface intersections, provide a very efficient 'funnel' for radiationless deactivation or for chemical transformation of the system (see for example the 'highlight' article by M. Klessinger[1]). As a consequence many of the 'textbook' models for the treatment of the photophysical and photochemical behaviour have been considerably refined. The purpose of this review is to outline the computational and experimental results that support this new view of photochemical reactivity.

In textbooks, the efficiency of internal conversion (IC) and intersystem crossing (ISC) is usually discussed in terms of the interaction between the vibrational energy levels of the ground and excited state potential energy surfaces using the Fermi Golden Rule. The traditional view of photochemical reactions (mainly due to the work of Van der Lugt and Oosteroff[2]) assumes that the absorption of a photon results in the generation of an excited state species (**M***). This intermediate represents the precursor of the photoproducts (**P**) which are generated *via* decay to the ground state. This decay was predicted to take place at an avoided crossing of the excited and ground state potential energy surfaces. At such an avoided crossing, if the energy gap is larger than few kJ mol^{-1}, **M*** will rapidly thermalyse and the decay probability will be determined by the Fermi Golden Rule. Accordingly, such processes are supposed to occur on the same timescale (several molecular vibrations) as fluorescence.

Modern experimental measurements and new computational techniques are now providing results that challenge such models for understanding organic photochemistry. Issues such as the efficiency of IC at a surface crossing, the competition with fluorescence when an excited state barrier is present, and the relationship between the molecular structure at the intersection and the structure of the photoproducts provide the intellectual motivation for the experimental and computational investigation of various photochemical reactions. The rate and the energy thresholds controlling IC can now be experimentally measured by exploiting the advances in laser spectroscopic techniques that have pushed the time resolution of various experimental techniques below the picosecond timescale. Thus, very fast IC processes and short excited state lifetimes can now be detected. For example, many detailed experiments are available in the photophysics and photochemistry of conjugated hydrocarbons in solution or isolated conditions. Femtosecond excited state lifetimes have been observed for simple dienes,[3] cyclohexadienes,[4] hexatrienes,[5] and in both free[6] and opsin-bound[7] retinal protonated Schiff bases. Experiments on isolated molecules in cold matrices or expanding jets have revealed the presence of 'thermally activated' fast radiationless decay channels in hexatrienes,[8] octatetraenes[9,10] and aromatic compounds (see refs. collected in ref. 11). While laser experiments provide information on the structure and energetics of the excited state potential energy surfaces controlling fast decay, more traditional photochemistry, such as quantum yield measurements, provide information on the molecular structure of the decay

Fernando Bernardi is Professor of Organic Chemistry at the University of Bologna. He received his degree in Industrial Chemistry at the University of Bologna in 1962 and studied with S.F. Boys in Cambridge (1969–1971). His research interests span all aspects of theoretical organic chemistry.

Massimo Olivucci is Ricercatore at the University of Bologna where he obtained his PhD in 1989. He was a post-doctoral fellow at King's College London 1989–1992. His research interests lie in the theoretical modelling of photochemistry.

Michael Robb is Professor of Chemistry at King's College London. He obtained his PhD from the University of Toronto in 1970 and was awarded the DSc from the University of London in 1988. His research interests lie in the development of MC-SCF methods and applications to chemical reactivity.

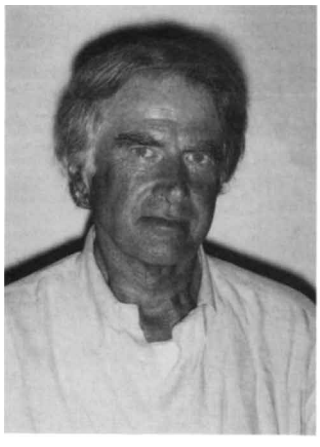

Fernando Bernardi

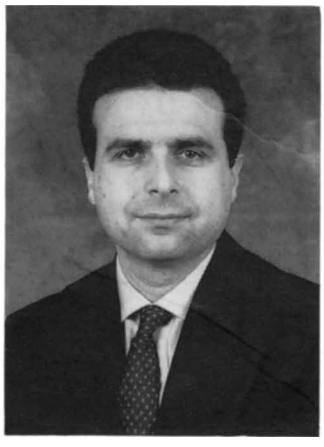

Massimo Olivucci

Michael Robb

channel and on the product formation paths The detailed characterisation of the stereo- and regio-chemistry of the primary photoproducts and transient intermediates, their quantum yields and the effect of specifically designed sterically and rotationally hindered reactants on these quantities[12] is now possible

An alternative view of photochemical reactions, that is consistent with recent experiments, was suggested more than 30 years ago by the physicist Edward Teller[13] at the 20th Farkas Memorial Symposium He suggested that it was the electronic factors that may play the dominant role in the efficiency of radiationless decay Teller made two general observations (*i*) In a polyatomic molecule the non-crossing rule, which is rigorously valid for diatomics, fails and two electronic states, even if they have the same symmetry, are allowed to cross at a conical intersection (*ii*) Radiationless decay from the upper to the lower intersecting state occurs within a single vibrational period when the system 'travels' in the vicinity of such intersection points On the basis of these observations, Teller proposed that conical intersections may provide a common and very fast decay channel from the lowest excited states of polyatomics In the field of photochemistry, Zimmerman[14] and Michl[15] were the first to suggest, independently, that certain photoproducts originate from IC at a conical intersection Zimmerman[14] and Michl[15] use the term 'funnel' for this feature

In this review we will show that, in agreement with the suggestions of Teller, Zimmerman and Michl, recent computational[11 16] work, when taken in conjunction with modern experimental studies, indicates that the radiationless decay process does not occur *via* an excited state intermediate in many cases, but rather through a conical intersection (*i e* an unavoided surface crossing) between excited and ground states Radiationless decay at a conical intersection implies that (*a*) the IC process will be 100% efficient (*i e* the Landau–Zerner[17] decay probability will be unity), (*b*) any observed retardation in the IC or reaction rate (*i e* the competition with flurorescence) must reflect the presence of some excited state energy barrier, which separates **M*** from the intersection structure and (*c*) in the case where the decay leads to a chemical reaction, the molecular structure at the intersection must be related to the structure of the photoproducts

2 The 'Physical Chemistry' of Conical Intersections

The precise nature of the molecular mechanism that controls radiationless decay in polyatomics is a problem that has intrigued photochemists and photophysicists for several decades An excited state species decays non-radiatively[18] *via* internal conversion (IC) to a state of the same spin multiplicity and *via* intersystem crossing (ISC) to a state of different spin multiplicity In textbooks, the efficiency of IC and ISC is usually discussed in terms of the interaction between the vibrational energy levels of the two potential energy surfaces using the Fermi Golden Rule,[18] see eqn (1)

$$k_{i\to f} = \frac{2\pi}{\hbar}\left\langle \Psi_i \middle| \hat{H} \Psi_f \right\rangle^2 \rho_E \qquad (1)$$

where $k_{i\to f}$ is the rate of transition from initial (*i*) to final (*f*) states, Ψ_i and Ψ_f are wavefunctions of initial and final states and ρ_E is the density of states Upon simplification this term reduces approximately to eqn (2)

$$k_{i\to f} \approx \langle \chi_i | \chi_f \rangle \beta^{\mathrm{ISC\ IC}} \qquad (2)$$

where $\langle \chi_i | \chi_f \rangle$ are Franck–Condon factors (*i e* vibrational overlaps) and $\beta^{\mathrm{ISC/IC}}$ is an electronic factor The efficiency of IC and ISC is often discussed in terms of Franck–Condon factors and $\beta^{\mathrm{ISC/IC}}$ is assumed to play a minor role

The Landau–Zener model provides an alternative semi-classical model for radiationless decay As shown by Desouter–Lecomte and Lorquet,[17] the probability of radiationless decay is given in eqn (3)

$$P = \exp[-(\pi/4)\xi] \qquad (3)$$

where ξ is the Massey parameter given as eqn (4)

$$\xi = \frac{\Delta E(\mathbf{q})}{\frac{h}{2\pi}|\mathbf{q}||g(\mathbf{q})|} \qquad (4)$$

where $\mathbf{q}$ is a vector of nuclear displacement coordinates The term $g(\mathbf{q})$ is the non-adiabatic coupling matrix element defined in eqn (6)

$$g(\mathbf{q}) = \left\langle \Psi_1 \middle| \frac{\partial \Psi_2}{\partial \mathbf{q}} \right\rangle \qquad (5)$$

while $|\mathbf{q}|$ is the magnitude of the velocity along the reaction path $\mathbf{q}$ and ΔE is the energy gap between the two states Ψ_1 and Ψ_2 Unless ΔE is less than a few kJ mol^{-1}, the decay probability is vanishingly small However, as we approach a point where the surfaces actually cross, the decay probability becomes unity

To understand the relationship between the surface crossing and photochemical reactivity, it is useful to draw a parallel between the role of a transition state in thermal reactivity and that of a conical intersection in photochemical reactivity

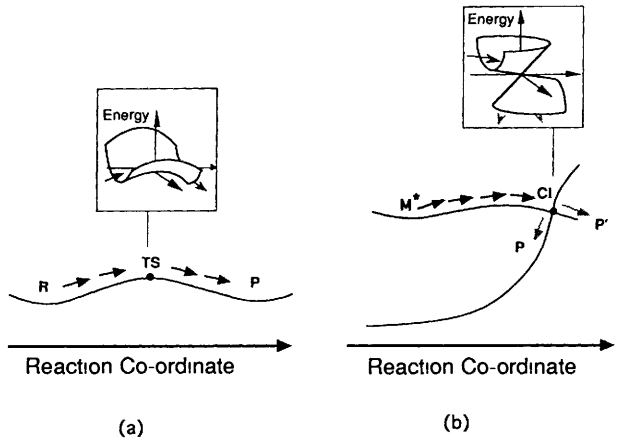

Scheme 1

In a thermal reaction, the transition state forms a dynamical bottleneck through which the reaction must pass on its way from reactants to products (Scheme 1a) A transition state separates the reactant and product energy wells along the reaction path A conical intersection (Scheme 1b) also forms a structural bottleneck that separates the excited state branch of the reaction path from the ground state branch The crucial difference between conical intersections and transition states is that, while the transition state must connect the reactant energy well to a *single* product well *via* a single reaction path, an intersection is a 'spike' on the ground state energy surface (see inset in Scheme 1b) and thus connects the excited state reactant to *two or more* products on the ground state *via* several ground state reaction paths The nature of the products generated following decay at a surface crossing will depend on the ground state valleys (reaction paths) that can be accessed from that particular structure

Theoretical investigations of surface crossings have required new theoretical techniques based upon the 'mathematical' description of conical intersections and we now briefly review the central theoretical aspects The double cone shape of the two intersecting potential energy surfaces can only be seen if the energies are plotted against two special internal geometric coordinates of the molecule ($\mathbf{x}_1$ and $\mathbf{x}_2$ in Scheme 2) The coordinate $\mathbf{x}_1$ is the gradient difference vector, given in eqn 6

$$\mathbf{x}_1 = \frac{\partial(E_1 - E_2)}{\partial \mathbf{q}} \qquad (6)$$

while $\mathbf{x}_2$ is the gradient of the interstate coupling vector, see eqn (7)

$$\mathbf{X}_2 = \left\langle \mathbf{C}_1 \left(\frac{\partial \mathbf{H}}{\partial \mathbf{q}} \right) \mathbf{C}_2 \right\rangle \qquad (7)$$

where $\mathbf{C}_1$ and $\mathbf{C}_2$ are the configuration interaction (CI) eigenvectors in a CI problem and $\mathbf{H}$ is the CI hamiltonian The vector $\mathbf{x}_2$ is

parallel to the non-adiabatic coupling given in eqn (5) These geometric coordinates form the so called 'branching space' As we move in this plane, away from the apex of the cone, the degeneracy is lifted (see Scheme 2a), and ground state valleys must develop on the lower cone In contrast, if we move from the apex of the cone along any of the remaining $n - 2$ internal coordinates (where n is the number of degrees of freedom of the molecule), the degeneracy is not lifted This space of $n - 2$ internal coordinates, the 'intersection space', is a hyperline consisting of an infinite number of conical intersection points (see Scheme 2b)

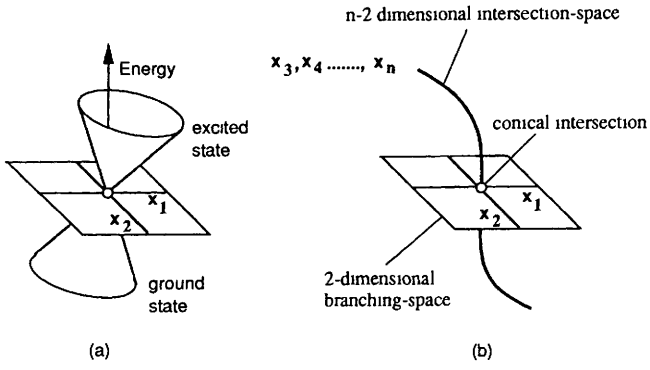

Scheme 2

Often the chemically relevant conical intersection point is located along a valley on the excited state potential energy surface Figure 1 illustrates a two-dimensional model example Here, two potential energy surfaces are connected *via* a conical intersection This intersection appears as a single point (CI) since the surfaces are plotted along the branching space ($\mathbf{x}_1, \mathbf{x}_2$) The intermediate **M*** is reached by relaxation from the Franck–Condon region (FC) and it is separated from the intersection point by a transition state (TS) In this case, the molecular structure of the intersection and the reaction pathway leading to it can be studied by computing the minimum energy path (MEP) connecting FC to **M*** and **M*** to CI using the standard intrinsic reaction coordinate (IRC) method [19] However, there are situations where there is no transition state connecting **M*** to the intersection point or where an excited state intermediate on the upper energy surface does not exist In such situations, mechanistic information must be obtained by locating the lowest lying intersection point along the $n - 2$ intersection space of the molecule

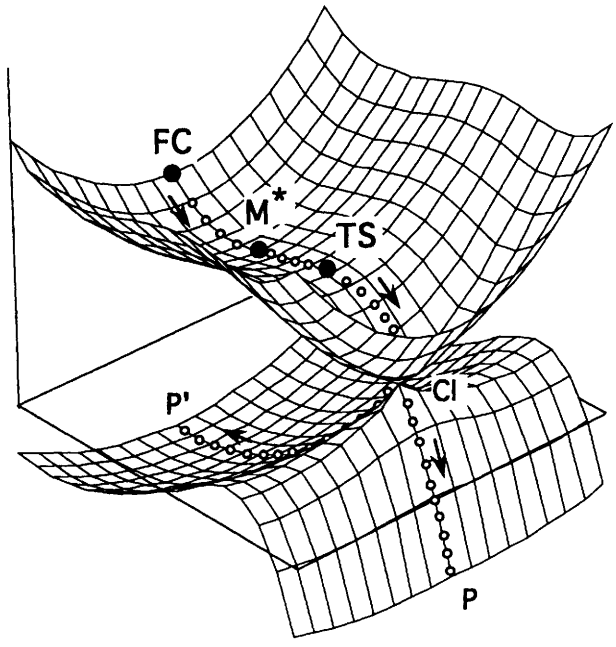

Figure 1 Model conically intersecting potential energy surfaces plotted along the branching space ($\mathbf{x}_1, \mathbf{x}_2$) The arrows indicate the direction of the minimum energy path connecting the FC point to the photoproducts **P** and **P'** **M*** is the excited state intermediate and TS is a transition state connecting **M*** to the conical intersection (CI)

The practical computation of the molecular structure of a conical intersection energy minimum can be illustrated by making an analogy with the optimization of a transition structure As illustrated in Scheme 1a, a transition structure is the highest energy point along the path joining reactants to products and the lowest energy point along all the $n - 1$ directions orthogonal to it One can optimize such a structure by minimising the energy in $n - 1$ orthogonal directions, and maximising the energy in the remaining direction corresponding to the reaction path The technique for locating the lowest energy intersection point[20] exploits the fact that the branching space directions $\mathbf{x}_1$ and $\mathbf{x}_2$ play a role analogous to the reaction path at the transition state Accordingly, the lowest energy point on a conical intersection is obtained by minimising the energy in the $n - 2$ dimensional intersection space ($\mathbf{x}_3, \mathbf{x}_4, \ldots, \mathbf{x}_n$), which preserves the degeneracy (see Scheme 2b)

The techniques outlined above provide information on the structure and accessibility of the intersection point, which controls the locus and efficiency of IC The evolution of ground state photoproducts following decay *via* such an IC channel requires a study of the possible ground state relaxation process Observe the shape of the ground state surface in the region of the conical intersection in Figure 1 The double cone in this case is 'elliptic' and two sides are steeper than the others This situation is typical of many cases and relaxation valleys develop more quickly in these directions We have recently implemented a method to locate and characterize all the relaxation directions that originate at the lower vertex of the CI cone [21] The MEP starting along these relaxation directions defines the ground state valleys, which determine the possible relaxation processes and the photoproducts This information is *structural* (*i e non-dynamical*) and provides insight into the mechanism of photoproduct formation from vibrationally 'cold' excited state reactants such as those encountered in many experiments where slow excited state motion or/and thermal equilibration is possible (in cool jets, in cold matrices and in solution)

In many cases, such structural or static information is not sufficient The excited state may not decay at the minimum of the conical intersection line Alternatively, the momentum developed on the excited state branch of the reaction coordinate may be sufficient to drive the ground state reactive trajectory along paths that are far from the ground state valleys In such cases, a dynamics treatment of the excited state/ground state motion is required For small systems, a parametrised potential can be developed and full semi-classical quantum dynamical treatment is possible [22] In our own work,[23] we have used classical dynamics with a parametrised hybrid quantum-mechanical/force-field (MMVB the molecular mechanics valence bond method) This method employs a 'direct' procedure for solving the equations of motion and avoids the tedious, and often unfeasible, parametrisation of an analytical expression of a multidimensional energy surface The trajectory-surface-hopping algorithm of Tully and Preston (see ref 23 for details) is used to propagate excited state trajectories on to the ground state in the region of a conical intersection

3 Reaction 'Funnels' in the Photochemistry of π–π^* and n–π^* States

The application of different spectroscopic techniques to low temperature samples of 'isolated' conjugated molecules has begun to provide very detailed information on the excited state dynamics of these organic systems In Figure 2 we illustrate the results of two different experiments The first experiment (Figure 2a) is due to Kohler and coworkers[10] who recorded the fluorescence lifetime of $S_1(2A_g)$ all-*trans*-octa-1,3,5,7-tetraene (all-*trans* OT) as a function of the temperature In this experiment the all-*trans* OT molecules are isolated in a molecular cavity of frozen hexane and do not interact with each other From Figure 2(a), one can see that, at temperatures above 200 K, the fluorescence lifetime drops dramatically indicating fast decay of the excited state molecules to the ground

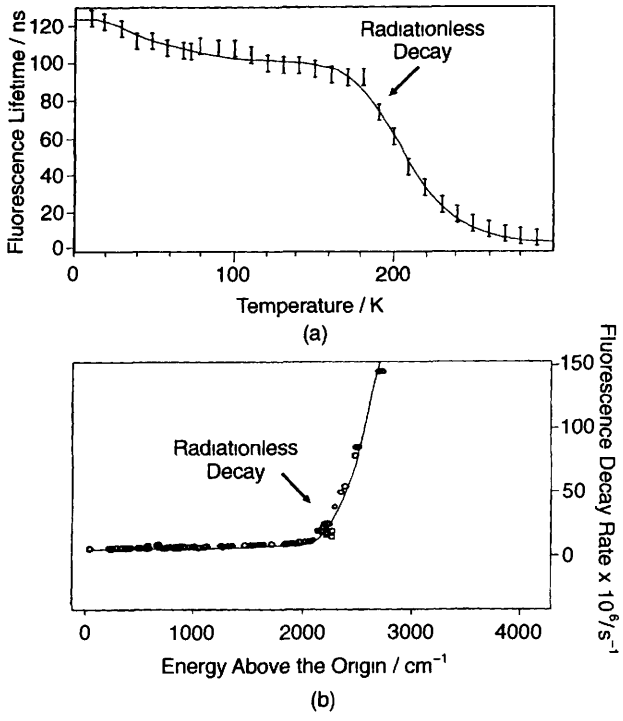

Figure 2 'Opening' of a fast radiationless decay channel in all *trans* octatetraene in (a) matrix isolated conditions (b) in a expanding cool jet

state This event was assigned to the opening of a thermally activated efficient radiationless decay channel with a barrier height of *ca* 1500 cm^{-1} (11 9 kJ mol^{-1}) The second experiment (Figure 2b) is due to Christensen, Yoshihara, Petek and coworkers,[9] who reported the fluorescence decay rate of S_1 all-*trans* OT molecules measured in free jet expansion as a function of the excitation energy These authors propose that *cis–trans* isomerisation is responsible for the radiationless decay channel, which opens up at *ca* 2100 cm $^{-1}$ (25 kJ mol $^{-1}$) excess energy The data from both experiments can be explained using the model surface shown in Figure Ja In both experiments the fluorescence lifetime decreases slowly and almost linearly by increasing the S_1 excess vibrational energy until an energy threshold is reached and a dramatic decrease in excited state lifetime is observed

Similar observations have been documented in other conjugated molecules In S_1 benzene there is a *ca* 3000 cm $^{-1}$ (35 9 kJ mol $^{-1}$) threshold for the disappearance of S_1 fluorescence (see ref 11) This observation is assigned to the opening of a very efficient, radiationless decay channel (termed 'channel 3') leading to the production of fulvene and benzvalene In S_1 cyclohexadiene, which is produced *via* a fast decay from the spectroscopic S_2 state, there must be a small barrier (*ca* 4 kJ mol $^{-1}$) to decay to S_0 since the photoproducts of the ring-opening reaction are detected a few picoseconds after initial excitation [4]

Ab initio CAS–SCF and multi-reference MP2 computations[11m16b] show that the topology of the first (π–π^*) excited state energy surface is indeed consistent with the model surface shown in Figure 1 (except for cyclohexadiene in which there is no transition structure between the excited state energy minimum and the intersection point[16a] Thus, the observed energy thresholds, which are well reproduced in theoretical computations, correspond to the energy barriers, which separate an excited state S_1 intermediate from a S_1/S_0 conical intersection point

The molecular system spends very little time in the neighbourhood of geometries characterised by conical intersections Thus, such geometries are not amenable to direct experimental observation and can only be derived from theoretical computations The optimized conical intersection structures for all-*trans* OT, S_1 benzene and S_1 cyclohexadiene intersections are collected in Figure 3 Comparison of these structures reveals common structural and electronic features Each structure contains a triangular

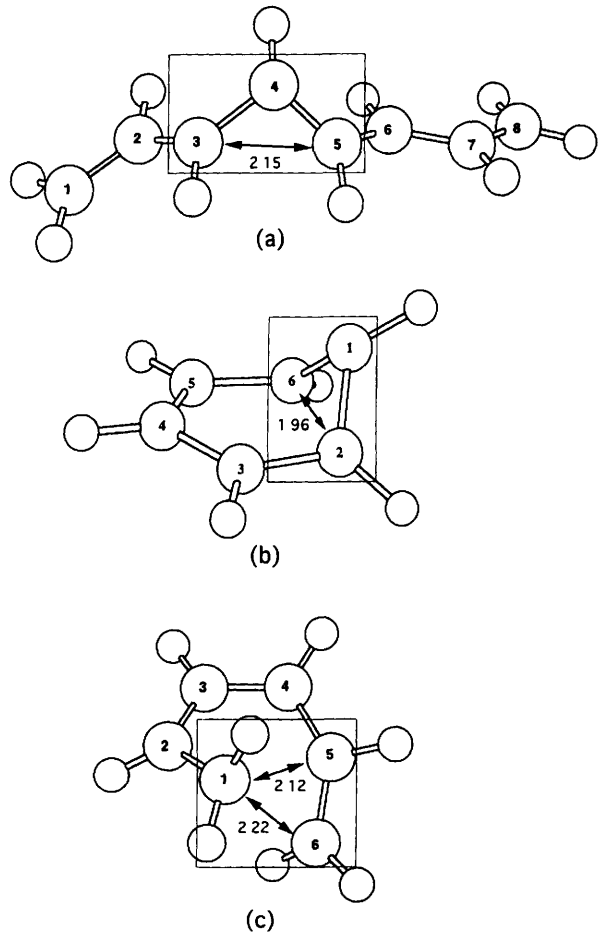

Figure 3 Structures of S_1/S_0 conical intersections in conjugated hydrocarbons showing the $-(CH)_3-$kink (framed) (a) all *trans* octatetraene, (b) benzene, (c) cyclohexadiene Interatomic distances are in Å

arrangement of three carbon centres corresponding to a $-(CH)_3-$kink of the carbon skeleton in all-*trans* OT[16b] and benzene[11] and to a triangular arrangement of the $-CH_2$ and $-CH-CH_2$ terminal fragments in cyclohexadiene [16a] The electronic structure in each case corresponds to three weakly interacting electrons in a triangular arrangement, which are loosely coupled to an isolated radical centre (this is delocalised on an allyl fragment in all-*trans* OT and benzene and localised in cyclohexadiene) This type of conical intersection structure appears to be a general feature of conjugated systems and has been documented in a series of polyenes and polyene radicals The electronic origin of this feature can be understood by comparison with H_3 where any equilateral triangle configuration corresponds to a point on the D_0/D_1 conical intersection in which the three H electrons have identical pairwise interactions

Moving from conjugated hydrocarbons to other classes of organic molecules, the electronic structure of the lowest lying intersection changes We now have detailed results on the Paterno–Buchi reaction,[16c], α,β-enones[16d], the oxadi-π-methane and [1,3]-acyl sigmatropic rearrangements of β,γ-enones,[16e] azocompounds (diazomethane[13g]) and photorearrangement of acylcyclopropenes to furans [16g] While hydrocarbon photochemistry typically involves a low energy covalent state, the photochemistry of bichromophoric (C=O and C=C) compounds is complicated by the competition between triplet $^3(\pi$–$\pi)$ pathways and singlet $^1(\pi$–$\pi)$ and triplet $^3(n$–$\pi)$ pathways The novel feature of our results is the discovery of points in the surface where all four states are degenerate This feature rationalises the singlet–triplet photochemistry in a novel way

The new features that arise in bichromophoric (C=O and C=C) compounds can be illustrated with the structure of the S_0/S_1 conical intersections found in α,β-enones In this case, the first singlet

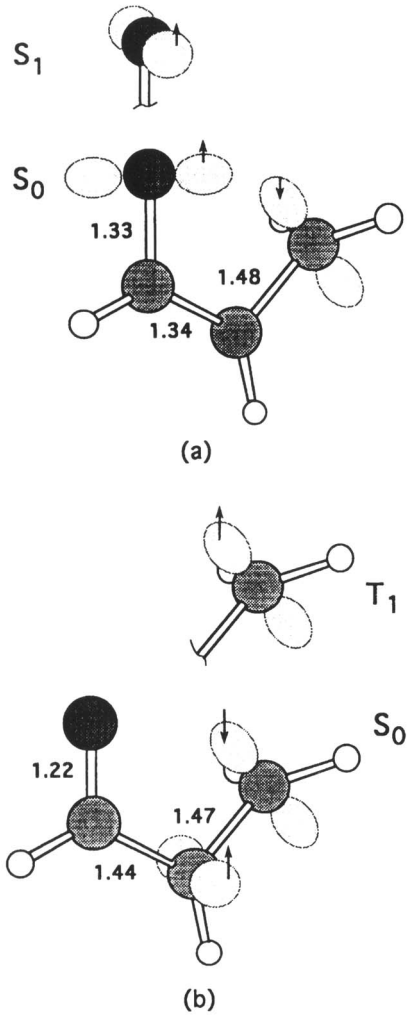

Figure 4 Low lying intersections in *cis* acrolein (a) $S_1(n-\pi^*)/S_0$ conical intersection (b) $T_1(\pi-\pi^*)/S_0$ triplet/singlet crossing

excited state is not a $\pi-\pi^*$ state but an $n-\pi^*$ state where the lone-pair orbital n becomes singly occupied This fact alone results in an electronic and molecular structure which is very different from the $-(CH)_3-$kink seen in conjugated hydrocarbons The case of *cis*-acrolein[16d] is instructive (see Figure 4a) The S_1/S_0 conical intersection has a 90° twisted terminal CH_2 and corresponds to a diradical with radical centres on CH_2 and O with a central C–C double bond (1 34 Å) This structure corresponds to a point of degeneracy between the $n-\pi^*$ and ground state because the radical centres do not interact with each other and with the central π–bond Thus, in this structure the S_0 state and the $^1(n-\pi^*)$ state differ only in a 90° *rotation* of the position of the singly occupied orbital on the oxygen Since the position of this radical centre is isolated from the CH_2 radical centre, the states have the same energy

The structure of the S_1/S_0 conical intersection in acrolein rationalises the observed wavelength dependent photochemistry of α,β-enones Direct irradiation with 310 nm light produces *cis–trans* double bond isomerisation exclusively In contrast, irradiation with 250 nm light produces a mixture of isomerisation and ring-closure products The 310 nm photochemistry comes from the enone T_1 triplet state Computations on acrolein demonstrate that this state is populated by ISC from the initial S_1 $(n-\pi^*)$ excited state molecule to a T_1 $(\pi-\pi^*)$ diradical intermediate the structure of which is shown in Figure 4b The $^3(\pi-\pi^*)$ diradical intermediate is not generated directly but involves decay through successive S_1/T_2 and a T_2/T_1 intersections The T_1 intermediate is located at a T_1/S_0 intersection and is the precursor of the photoproducts, which are generated *via* a slow ISC process The stability and structure of this diradical correlates nicely with the observed phosphorescence[24] and lack of production of the four-membered ring oxetene upon >300 nm irradiation [25] In fact, while the two radical centres are located on two vicinal carbons, the carbonyl bond is fully formed Consequently, relaxation to the S_0 state can only result in α,β-enone formation structure *via cis–trans* motion The production of oxetane requires a very different decay point, which is assigned to the S_1/S_0 conical intersection described above The fact that 250 nm radiation is required for populating this decay channel is consistent with the fact that this is located at least 40 kJ mol $^{-1}$ above the initial S_1 structure

4 Butadiene Photochemistry: Beyond the Woodward–Hoffman rules

The cyclisation of butadienes and ring-opening of cyclobutenes are textbook examples of pericyclic reactions The stereochemistry of both thermal and photochemical pericyclic reactions can be predicted on the basis of the Woodward–Hoffman (WH) rules [18] Despite the fact that the success of these rules has been demonstrated in many cases, it is not obvious why they work in the case of the photochemistry of polyenes The WH rules predict the stereochemistry of the motion on the (HOMO–LUMO singly excited) $^1B_2$ spectroscopic state (see Figure 5a) However, the spectroscopic investigation[3,5] of short polyenes shows that after photoexcitation these systems decay to a lower lying doubly excited ($2A_1$) state Thus, the photoproducts must originate from this state *via* IC Why is the 'disrotatory' stereochemistry predicted for the spectroscopic state of *s-cis* butadiene not lost on the $2A_1$ state? Further, while a rigid disrotatory stereochemistry has been experimentally observed for the *s-cis* butadiene ring-closure, Leigh *et al* [26] have demonstrated that the reverse photoreaction, the ring-opening of cyclobutene, occurs with a low degree of stereospecificity

About 20 years ago Van der Lugt and Oosteroff[2] proposed that along distinguished disrotatory and conrotatory ring-closure coordinates, the $2A_1$ state has two deep minima The observed disrotatory stereochemical preference was then explained on the basis of a higher rate of IC at the disrotatory $2A_1$ minimum (see arrows in Figure 5a) owing to a substantially smaller excited state/ground state energy gap in this point The recent computational re-investigation of the interplay between the $2A_1$ dark state potential energy surface, the $1B_2$ surface and the $1A_1$ ground state surface of *s-cis* butadiene rationalises its photo-stereochemistry[16h] In Figure 5b we show the energy profiles along the reaction paths computed for the first two excited states of *s-cis* butadiene Upon relaxation from the FC region, the photoexcited molecule undergoes a barrierless relaxation leading ultimately to decay to the $1A_1$ ground state There are two successive intersection points involved in the relaxation process The first intersection occurs between the spectroscopic $1B_2$ state and the dark $2A_1$ state and is located in the vicinity of the FC region This is consistent with spectroscopic studies on isoprene (2-methylbutadiene),[3] which indicates that the $1B_2$ state is depopulated on a timescale of 10 fs owing to fast internal conversion to the nearby $2A_1$ state The second intersection involves a conical intersection between the $2A_1$ and the $1A_1$ state, which will be entered after $2A_1$ geometric relaxation Thus, photoproduct formation occurs after $2A_1$ decay following solvent cooling of the initially hot molecule

The $1B_2$ path, which describes the relaxation from the FC region (see arrows in Figure 5b), involves a disrotatory motion of the terminal methylenes in agreement with the prediction of the WH rules However, both a disrotatory and a conrotatory reaction path exist on the $2A_1$ potential energy surface, which ends in the same $2A_1/1A_1$ crossing region However, while the disrotatory path is barrierless the conrotatory path has a barrier (due mainly to steric effects) and it is located 30 kJ mol $^{-1}$ higher in energy Thus, the (energetically preferred) structural evolution of the system along the $2A_1$ energy surface will also be disrotatory but for a reason unrelated to the WH theory Simply, the conrotatory motion on the $2A_1$ surface is hindered by a barrier The original Van der Lugt and Oosteroff model (arrows in Figure 5a) can now be refined Our computations and experimental work indicate the existence of a disrotatory $1B_2/2A_1$ crossing in butadienes However, there are no

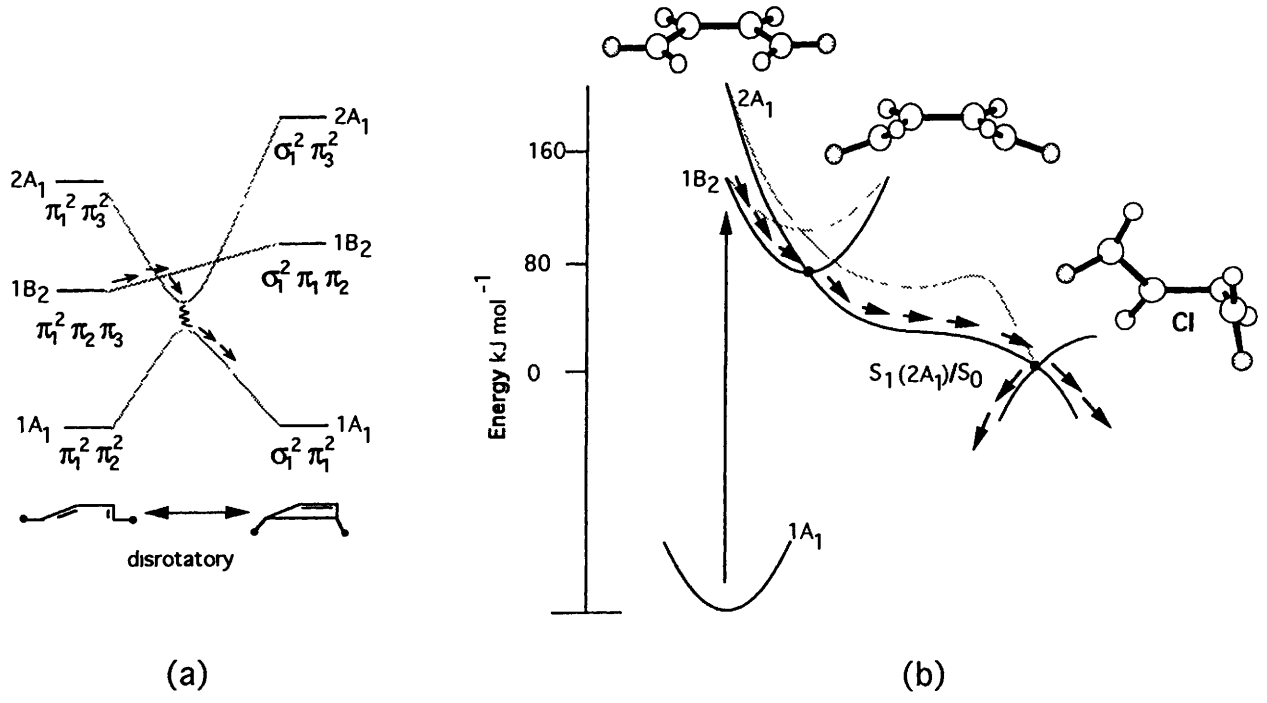

Figure 5 Butadiene photochemistry (a) WH state correlation diagram The arrows represent the Van der Lugt and Oosteroff mechanism (b) Computed MEP from the S_2 ($1B_2$) FC structure of *s cis* butadiene to the S_1 ($2A_1$)/S_0 conical intersection Full lines and light lines represent the energy profile along the disrotatory and conrotatory MEP, respectively The terminal hydrogen atoms in the structures have been highlighted to indicate the stereochemistry

true $2A_1$ minima and the lowest energy point on the $2A_1$ state is a conical intersection

Direct irradiation of *s-cis* butadienes is known to yield a mixture of *cis–trans* isomerisation and cyclisation photoproducts[27] In a 20 K matrix Squillacote *et al* have measured the ratios of double-bond *cis–trans* isomerisation, *s-cis*>*s-trans* isomerisation, ring-closure and reactant back-formation The structure of the computed $2A_1/1A_1$ conical intersection and the energy profiles of the four relaxation paths that begin at the apex of this conical intersection are shown in Figure 6 Neglecting the effect of dynamical factors, which may, in principle, control the efficiency of the different relaxation processes, it is obvious that double-bond *cis–trans* isomerisation, ring-closure and reactant back-formation will be competitive We have not been able to locate a path leading to the cyclopropylmethylene diradical, which is a precursor of bicyclobutane This observation is consistent with the fact that this product has not been seen experimentally Our theoretical prediction, which suggests that the photoreactivity of *s-cis* butadiene involves simultaneous twisting motion about the central C–C bond and one of the original double bonds (see Figure 5b), has been experimentally tested by Leigh *et al* using a series of C–C ring-locked butadienes [12] Their experiments show that the yield for double-bond isomerisation is indeed affected by the size of the ring blocking the C–C *s-cis*>*s-trans* rotation

The reaction paths illustrated in Figures 5 and 6 also provide an explanation for the lack of stereochemistry observed in cyclobutene (CB) ring-opening reactions [26] (The WH rules predict a disrotatory stereochemistry) The experimental observations can be explained by assuming that the CB ring opens on the $1B_2$ state In this way CB photolysis would yield $1B_2$ *s-cis* butadiene, which decays to the dark $2A_1$ state following the pathway illustrated in Figure 5b The CB final photoproducts must originate *via* decay at the same $2A_1/1A_1$ conical intersection and will follow the relaxation paths shown in Figure 6 It is then obvious that, since decay at this point involves *concurrent* butadiene formation and double-bond *cis–trans* isomerisation, the production of a stereospecific (disrotatory) ring-opening product is impossible Thus, the loss of stereochemistry is due to the *unavoidable* concurrent *cis–trans* isomerisation and butadiene formation

5 Towards a Dynamic View of Photochemical Processes: Benzene and Azulene

In our preceding discussion of butadiene photochemistry, we have shown how excited state and ground state relaxation paths can provide structural (*i e* non-dynamical) information on the mechanism of product formation associated with radiationless deactivation A more realistic picture of these processes requires the description of the reaction dynamics obtained from the computation and analysis of non-adiabatic trajectories We now illustrate this point with some results on benzene and azulene

The lifetime of the S_1 state of vapour phase benzene drops dramatically when the vibrational excess energy overcomes a *ca* 3000 cm^{-1} (35 9 kJ mol^{-1}) barrier In contrast, recent spectroscopic investigations have demonstrated that the S_1 state of the pseudo-aromatic molecule azulene has a sub-picosecond lifetime arising from a nearly barrierless fast deactivation process Our recent *ab initio* computations[11 16] rationalise these data and have confirmed that in both molecules a S_1/S_0 conical intersection occurs on the S_1 potential energy surface

Non-adiabatic dynamics from benzene[23] and azulene[16] S_1 states give new insight into the quantum yield of prefulvene in the case of benzene, and suggest that one may observe coherent vibrations on the ground state of azulene In Figure 7 we show that the S_1 potential energy surfaces of benzene and azulene have different shapes in the region of the conical intersections For S_1 benzene there is a substantial barrier separating an excited state intermediate from the conical intersection region In contrast, azulene shows a 'sloped' conical intersection, which is slightly higher than the intermediate region Our dynamics studies have been carried out with the MMVB technique discussed in ref 23 Comparison of the MMVB energy and molecular structures of benzene and azulene with the corresponding *ab initio* parameters (see Figure 7) indicates a good qualitative agreement The computed non-adiabatic dynamics are thus expected to be qualitatively correct

In the case of benzene our objective was to understand the origin of the very low quantum yield (*ca* 0 02) for the production of benzvalene Figure 7(a) shows that there is an S_1 transition structure with a geometry that is virtually identical to the optimized intersection Thus, there will be two possible types of trajectory that pass

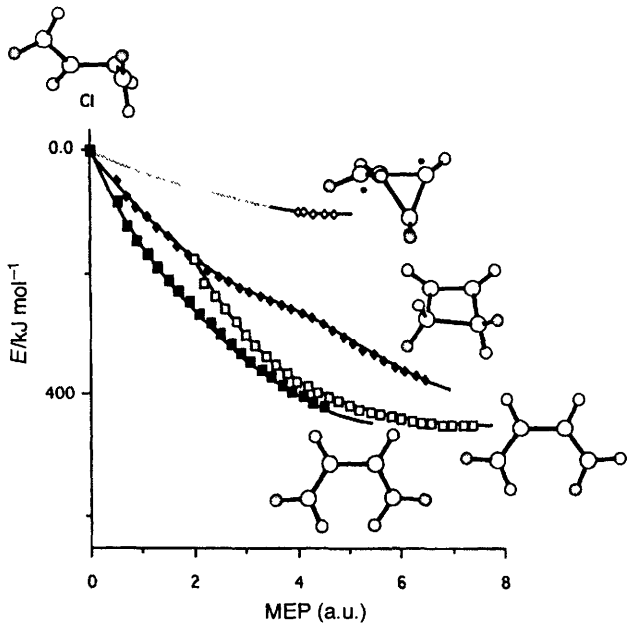

Figure 6 Energy profiles along the computed MEP describing the relaxation from the S_1/S_0 conical intersection point to the *s-cis* butadiene photoproducts. The terminal hydrogen atoms in the structures have been highlighted to indicate the stereochemistry.

through the conical intersection region: trajectories that follow the reaction path between the S_1 minimum and the prefulvene structure and trajectories that return to the S_0 minimum after a surface hop. The quantum yield corresponds to the ratio of the numbers of trajectories leading to the prefulvene as a function of the total. In our simulation, the initial conditions were designed to select trajectories approaching the intersection region. There are two variables associated with the initial conditions: (*a*) the value of the initial kinetic energy (momentum) along the reaction path and (*b*) the value of the initial vibrational kinetic energy randomly distributed among the normal modes orthogonal to the reaction path.

The effect of the initial momentum along the reaction path is shown in Table 1, which lists the percentage of trajectories that

Table 1 Quantum yield of prefulvene as a function of the initial momentum (excess energy) along the reaction path

Excess energy kJ mol⁻¹	Hopped trajectories (%)	Prefulvene yield (%)
12.9	48	0.0
22.5	100	0.0
25.1	100	2.7
27.6	100	3.1
32.6	100	2.0
37.7	100	2.7
41.8	100	11.3
48.5	100	22.3

hopped during the simulation, and the percentage that terminated in the prefulvene region, for a range of excess kinetic energies. The very small computed yield of prefulvene shows a general increase as the kinetic energy rises. The experimental quantum yield at 253 nm is 0.016 which rises slightly to 0.037 at 237 nm. These results are remarkable for two reasons. First, we manage to reproduce the characteristic low quantum yield observed experimentally. Secondly, we find that the dynamics associated with passage through the conical intersection can be interpreted using simple classical arguments. If the excess energy is directed along the reaction coordinate leading to prefulvene, the quantum yield increases. If the excess kinetic (vibrational) energy is directed orthogonal to the reaction coordinate the quantum yield decreases (see Table 2). Thus, sampling a larger area of the potential surface at higher kinetic energies, produces trajectories that are no longer confined to the bottom of the reaction 'valley'. Rather, the initial kinetic energy will be distributed into a variety of vibrations, and not just be directed toward the prefulvene region.

The anomalous fluorescence of azulene – emission from S_2 rather than S_1 – was first recognised by Beer and Longuet-Higgins forty years ago (see refs. in 16*i*). Femtosecond laser studies and spectroscopic linewidth measurements have now established that complete internal conversion from S_1 to the ground state takes place in less than a picosecond. *Ab initio* computations show how such ultra-fast decay can be explained by the S_0/S_1 conical intersection represented in Figure 7(b). The molecular dynamics studies suggest that the decay can take place before a single oscillation

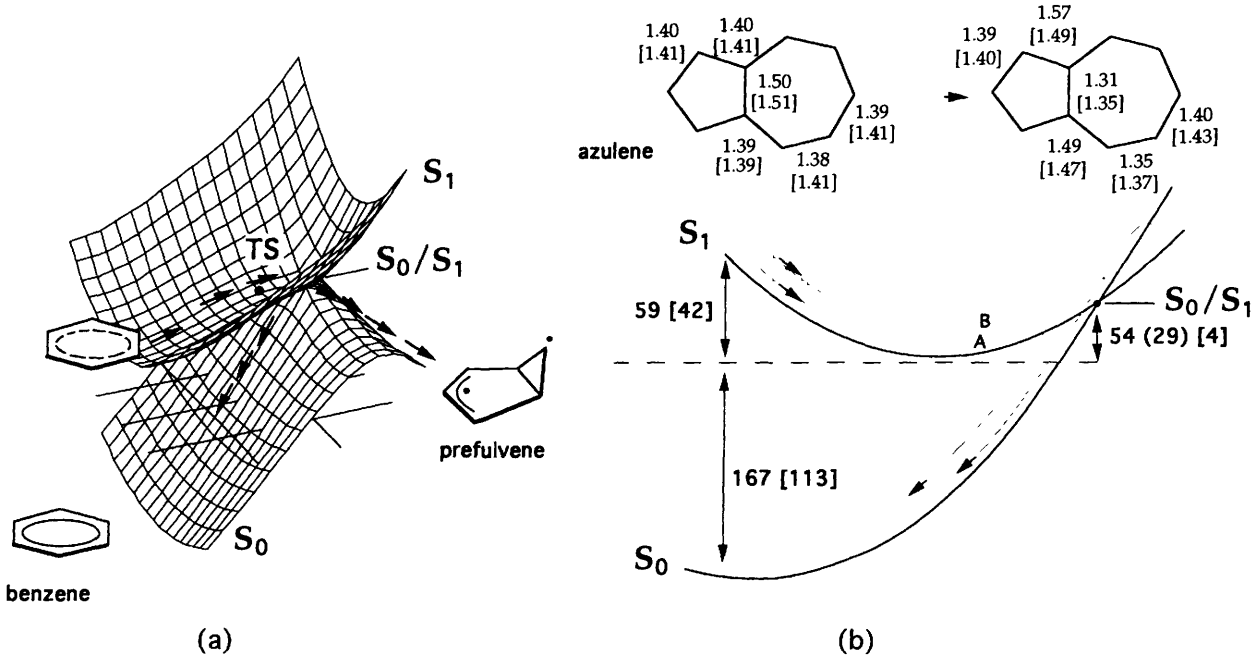

Figure 7 Conically intersecting potential energy surfaces in benzene and azulene. (a) Shape of the S_1 and S_0 energy surfaces in benzene. The arrows represent the MEP connecting S_1 benzene to the product well *via* the conical intersection. (b) S_1 and S_0 energy profiles along the S_1 path from the FC structure of azulene. The *ab initio* and MM–VB (in square brackets) geometrical parameters and energies are reported in Å and kJ mol^{-1}, respectively.

Table 2 Quantum yield of prefulvene as a function of the initial vibrational kinetic energy (ΔE_{lim}) randomly distributed among the normal modes orthogonal to the reaction path The effect is shown for two values of the initial momentum along the reaction path (excess energy)

$\Delta E_{lim}/E_h$[a]	Prefulvene yield (%)	
	Excess energy (27 6 kJ mol $^{-1}$)	Excess energy (43 1 kJ mol $^{-1}$)
0 00	12 7	11 3
0 002	1 21	6 8
0 003	2 0	10 5
0 004	2 3	8 6
0 005	0 8	7 4
0 006	0 4	7 0
0 007	0 4	5 1
0 008	0 0	4 7

E_h = Hartree units (1 E_h = 2626 kJ mol $^{-1}$)

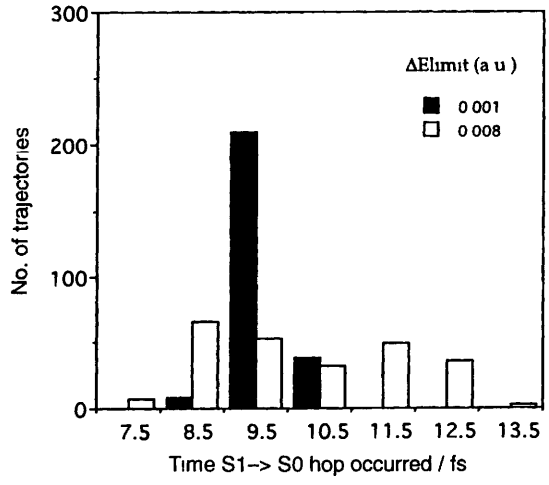

Figure 8 Azulene dynamics simulations distribution of hop times with small and large initial vibrational excess energies (ΔE_{lim})

through the intersection space is completed The results of this simulation are summarised in Figure 8 The average time taken to reach the hopping region is always *ca* 10 fs and it is the time dispersion that increases with the available kinetic energy at the hop At low kinetic energies (0 001 a u), nearly all (observe the single peak in Figure 8) of the surface hops occur within the first half vibrational-period of their excited state lifetime (trajectory A in Figure 7b) At higher initial energies there is a much wider spread of crossing times with two clear peaks, corresponding to hops earlier and later than those observed at lower energy The second peak, therefore, corresponds to molecules that decay after having completed the first half of a vibration along the relaxation coordinate (trajectory B in Figure 7b)

6 Concluding Remarks

Excited state reactivity is controlled by three factors (*a*) the presence and magnitude of barriers in the excited state branch of the reaction coordinate, (*b*) the dynamics of IC or ISC as the system returns to the ground state and (*c*) the nature of ground state reaction pathways that are populated following IC or ISC The concept of the 'photochemical funnel' introduced by Zimmerman[14] and Michl[15] can now be substantiated *via* both computational and experimental investigations Advances in computer and laser technology, and the introduction of new computational and experimental methodologies are yielding a new mechanistic picture of photochemical reactions This picture is based upon the idea that single or successive low-lying intersections provide the bottlenecks controlling the evolution of a photoexcited molecule from the FC region to the photoproduct valleys Both theory and experiment now indicate that such intersection mechanisms are a general feature in photochemical reactivity problems

Acknowledgements This research has been supported in part by the EPSRC (UK) under grant numbers GR/J25123 GR/H58070 and GR/K04811 We are also grateful to NATO for a travel grant (CRG 950748)

7 References

1 See references collected in M Klessinger, *Angew Chem Int Ed Engl* ,1995, **34**, 549
2 W T A M Van der Lugt and L J Oosteroff, *J Am Chem Soc* 1969, **91**, 6042
3 M O Trulson and R A Mathies, *J Phys Chem* 1990, **94**, 5741
4 See (*a*) P J Reid, S J Doig, S D Wickham and R A Mathies, *J Am Chem Soc* , 1993, **115**, 4754 and references cited therein, (*b*) S Pullen, L A Walker II, B Donovan and R J Sension, *Chem Phys Lett* , 1995 **242**, 415
5 D R Cyr and C C Hayden, *J Chem Phys* , 1996, **104**, 771
6 H Kandori, Y Katsuta, M Ito and H Sasabe, *J Am Chem Soc* , 1995, **115**, 2669
7 Q Wang, R W Schoenlein, L A Peteanu, R A Mathies and C V Shank, *Science*, 1994, **266**, 422
8 H Petek, A J Bell, R L Christensen and K Yoshiara, *SPIE*, 1992, **1638**, 345
9 H Petek, A J Bell, Y S Choi, K Yoshiara, B A Tounge and R L Christensen, *J Chem Phys* , 1993, **98**, 3777
10 B E Kohler, *Chem Rev* , 1993, **93**, 41
11 I J Palmer, I N Ragazos, F Bernardi, M Olivucci and M A Robb, *J Am Chem Soc* , 1992, **115**, 673
12 W J Leigh and A Postigo, *J Chem Soc Chem Commun* , 1993, 1836
13 E Teller, *Isr J Chem* , 1969, **7**, 227
14 H E Zimmerman, *J Am Chem Soc* , 1966, **88**, 1566
15 J Michl, *J Mol Photochem* , 1972, 243
16 (*a*) P Celani, S Ottani, M Olivucci, F Bernardi and M A Robb, *J Am Chem Soc* , 1994, **116**, 10141, (*b*) P Celani, M Garavelli, S Ottani, F Bernardi, M A Robb and M Olivucci, *J Am Chem Soc* , 1995, **117**, 11584, (*c*) I J Palmer, I N Ragazos, F Bernardi, M Olivucci and M A Robb, *J Am Chem Soc* , 1994, **116**, 2121, (*d*) M Reguero, M Olivucci, F Bernardi and M A Robb, *J Am Chem Soc* , 1994, **116**, 2103, and references cited therein, (*e*) S Wilsey, M J Bearpark, F Bernardi, M Olivucci and M A Robb, *J Am Chem Soc* , 1996, **118**, 176, (*f*) see N Yamamoto, F Bernardi, A Bottoni, M Olivucci, M A Robb and S Wilsey *J Am Chem Soc* , 1994, **116**, 2064, and references cited therein, (*g*) S Wilsey, M J Bearpark, F Bernardi, M Olivucci and M A Robb, *J Am Chem Soc* , 1996, in press, (*h*) P Celani, F Bernardi, M Olivucci and M A Robb, *J Chem Phys* , 1995, **102**, 5733, (*i*) M J Bearpark, F Bernardi, S Cliffort, M Olivucci, M A Robb, B R Smith and T Vreven, *J Am Chem Soc* , 1996, **118**, 169
17 M Desouter Lecomte and J C Lorquet, *J Chem Phys* , 1977, **71**, 4391
18 A Gilbert and J Baggott, 'Essentials of Molecular Photochemistry', Blackwell Scientific Publications, Oxford, 1991
19 M L McKee and M Page, in 'Reviews in Computational Chemistry', ed K B Lipkowiz and D B Boyd, 1993, **4**, 35
20 I N Ragazos, M A Robb, F Bernardi and M Olivucci, *Chem Phys Lett* , 1992, **197**, 217 M J Bearpark, M A Robb and H B Schlegel, *Chem Phys Lett* , 1994, **223**, 269
21 P Celani, M A Robb, M Garavelli, F Bernardi and M Olivucci, *Chem Phys Lett* , 1995, **243**, 1
22 H Koppel, W Domcke and L S Cederbaum, *Adv Chem Phys* , 1984, **57**, 59
23 B R Smith, M J Bearpark, M A Robb, F Bernardi and M Olivucci, *Chem Phys Lett* , 1995, **242**, 27
24 R S Becker, K Inuzuka and J King, *J Chem Phys* , 1970, **52**, 5164
25 L E Friedrich and G B Schuster, *J Am Chem Soc* , 1972, **94**, 1193
26 W J Leigh and K Zeng, *J Am Chem Soc* , 1991, **113**, 2163
27 M Squillacote and T C Sample, *J Am Chem Soc* , 1990, **112**, 5546